

RESEARCH ARTICLE

Open Access



Alteration of gray matter texture features over the whole brain in medication-overuse headache using a 3-dimensional texture analysis

Zhiye Chen^{1,2,3†}, Xiaoyan Chen^{3†}, Zhiqiang Chen^{4,5†}, Mengqi Liu^{1,2}, Huiguang He^{4,5,6*}, Lin Ma^{1*} and Shengyuan Yu^{3*} 

Abstract

Background: Imaging studies have provided valuable information in understanding the headache neuromechanism for medication-overuse headache (MOH), and the aim of this study is to investigate altered texture features of MR structural images over the whole brain in MOH using a 3-dimensional texture analysis.

Methods: Brain three-dimensional T1-weighted structural images were obtained from 44 MOH patients and 32 normal controls (NC). The imaging processing included two steps: gray matter (gray images) segment and a 3-dimensional texture features mapping. Voxel-based gray-level co-occurrence matrix (VGLCM) was performed to measure the texture parameters mapping including Contrast, Correlation, Energy, Entropy and inverse difference moment (IDM).

Results: The texture parameters of increased Contrast and Entropy, decreased Energy and IDM were identified in cerebellar vermis of MOH patients compared to NCs. Increased Contrast and decreased Energy were found in left cerebellum. Increased Correlation located in left dorsolateral periaqueductal gray (L-dIPAG), right parahippocampal gyrus (R-PHG), and left middle frontal gyrus (L-MFG) and decreased Correlation located in right superior parietal lobule (R-SPL). Disease duration was positively correlated with Contrast of vermis and negatively correlated with Correlation of R-SPL. HAMD score was negatively correlated with Correlation of R-PHG. MoCA score was positively correlated with Correlation of R-SPL.

Conclusion: The altered textures in gray matter related to pain discrimination and modulation, affective and cognitive processing were helpful in understanding the pathogenesis of MOH. Texture analysis using VGLCM is a sensitive and efficient method to detect subtle gray matter changes in MOH.

Keywords: Magnetic resonance imaging, Medication-overuse headache, Migraine, Texture analysis, Voxel-based gray-level co-occurrence matrix

Background

Medication-overuse headache (MOH) is a secondary chronic headache in patients with a pre-existing primary headache disorder caused by regular overuse of acute or symptomatic headache medication for more than

3 months [1]. MOH was one of the most prevalent neurological disorders to cause disability [2]. Medication withdrawal was the primary treatment but only a few patients may achieve improvement [3]. However, the mechanism of MOH generation still remains unclear. Imaging studies have played a role in elucidating the pathophysiological changes of MOH by finding alteration in various aspects of pain processing and reward system [4]. In the published documents, the common MRI technique about headache included conventional T2WI [5], advanced brain structure segment [6–8],

* Correspondence: huiguang.he@ia.ac.cn; cjr.malin@vip.163.com; yusy1963@126.com

†Equal contributors

⁴Research Center for Brain Inspired Intelligence, Institute of Automation, Chinese Academy of Sciences, Beijing 100190, China

¹Department of Radiology, Chinese PLA General Hospital, Beijing 100853, China

³Department of Neurology, Chinese PLA General Hospital, Beijing 100853, China

Full list of author information is available at the end of the article

resting-state functional MRI [9], and diffusion kurtosis imaging (DKI) [10], which provided much more valuable information to understand the headache neuromechanism. However, this advanced MRI technique may consume much more labour and time, and some functional test might also be influenced by some uncontrolled state such as motion and emotion.

Texture features are the intrinsic properties of images, and reflects the degree of gray distribution, contrast, spatial distribution and other image characteristics [11]. Texture analysis plays a key role in the image analysis, and it could make the invisible intrinsic image characteristics visible [12]. Recent studies presented that texture analysis had widely been applied in the clinical practice, such as rectal cancer [13, 14], hepatic hemangioma [15], mild cognitive impairment [16], glioblastoma [17], and etc. In our previous study [18], we performed a pilot texture feature analysis for periaqueductal gray (PAG) using a 2-dimensional gray-level co-occurrence matrix (2D-GLCM) and primary results suggested increased Contrast presented in MOH patients. However, 2D-GLCM might be influenced by some factors, such as the size of the step in pixels and the direction of the step, and manual measurement. Therefore, it was limited in the clinical practice. In recent documents [19, 20], 3-dimensional (3D) texture analysis technique were reported, and it had some valuable merits, such as voxel-based analysis over the whole brain, and not influenced by the size and the direction. However, the main limit for the previous study was the calculation time, which would need 15–30 min for one texture map [19]. Therefore, the optimization of the 3D texture calculation would improve the clinical application of this texture technique.

In the current study, we hypothesize that there's altered texture feature of gray matter in MOH patients. To address this hypothesis, we prospectively acquired high resolution structural images from 44 MOH patients and 32 normal controls (NC). Secondly, voxel-based GLCM optimize and improve the texture calculation efficacy. Lastly, the five texture feature maps were generated and performed with voxel-based analysis over the whole brain to identify the brain regions with abnormal texture changes in MOH.

Methods

Subjects

The current study was approved by the local institutional review board, and Written informed consent was obtained from all participants according to the approval of the ethics committee. Forty-four MOH patients were enrolled from the International Headache Center, Department of Neurology, Chinese PLA General Hospital. The inclusion criteria should be fulfilled as following: 1) diagnosis of 8.2 MOH, and 1.1 and 1.2 migraine based on the

International Classification of Headache Disorders, third Edition (beta version) (ICHD-III beta) [1]; 2) no migraine preventive medication used in the past 3 months. The exclusion criteria were the following: 1) with any chronic disorders, including hypertension, diabetes mellitus, cardiovascular diseases, cerebrovascular disorders, neoplastic diseases, connective tissue diseases, other subtypes of headache, chronic pain other than headache, severe anxiety or depression preceding the onset of headache, psychiatric diseases, etc.; 2) with alcohol, nicotine, or other substance abuse; 3) with psychotic disorder and regular use of a psychoactive or hormone medication. Thirty-two normal controls (NCs) were recruited from the hospital's staff and local community. NCs should never have had any primary headache disorders or other types of headache in the past year, and the exclusion criteria was the same with MOH's exclusion criteria. General demographic and headache information were registered and evaluated in our headache database. All the patients were given with the Visual Analogue Scale (VAS). All the participants were evaluated by the Hamilton Anxiety Scale (HAMA) [21], the Hamilton Depression Scale (HAMD) [22], and the Montreal Cognitive Assessment (MoCA) Beijing Version (<http://www.mocatest.org>). All imaging protocols were identical for all the subjects. Alcohol, nicotine, caffeine, and other substances were avoided for at least 12 h before MRI examination.

MRI acquisition

All MRI data were acquired on a GE 3.0 T MR system (DISCOVERY MR750, GE Healthcare, Milwaukee, WI, USA) and a conventional eight-channel quadrature head coil was used. Firstly, conventional T2-weighted imaging (T2WI) and T1 fluid-attenuated inversion recovery (T1-FLAIR) weighted imaging were acquired to exclude the subjects with obvious structural damage and T2-visible lesion. Secondly, the brain structural images were obtained by a three-dimensional T1-weighted fast spoiled gradient recalled echo (3D T1-FSPGR) sequence generating 180 contiguous axial slices [TR (repetition time) = 6.3 ms, TE (echo time) = 2.8 ms, flip angle = 15°, FOV (field of view) = 25.6 cm × 25.6 cm, Matrix = 256 × 256, NEX (number of acquisition) = 1].

MR image processing

All the data were processed using Statistical Parametric Mapping 12 (SPM 12) (<http://www.fil.ion.ucl.ac.uk/spm/>), FSL (v5.0) (<https://fsl.fmrib.ox.ac.uk/fsl/fslwiki/>) and MA TLAB 7.6 (The Mathworks, Natick, MA, USA). The imaging processing included two steps: gray matter (gray images) segment and a 3-dimensional texture features mapping.

First step was performed with the following procedures: (1) the raw brain structural images (3D T1-FSPGR) (Fig. 1a) were normalized into MNI space, and the normalized T1 images were obtained (Fig. 1b), which were gray images while not probability images. (2) The normalized T1 images were performed with brain extraction using FSL (v5.0) tool to delete the non-brain tissue, and obtained a good brain T1 images (Fig. 1c). (3) The normalized T1 images were performed with DARTEL segment [23], and gray matter images (tissue probability images) were obtained (Fig. 1d). (4) The gray matter images were performed with binary mask creation, and the gray matter mask was acquired (Fig. 1e). (5) The T1 images without non-brain tissue (Fig. 1c) were masked with the previous gray matter mask, and the final gray matter of the brain (gray images) was obtained (Fig. 1f).

Following processing was the 3-dimensional texture maps generation. All the texture maps were generated by improved voxel-based gray-level co-occurrence matrix (VGLCM) method [20], and the texture parameters included Contrast, Correlation, Energy (angular second moment, ASM), Entropy and Inverse Difference Moment (IDM) [15, 18]. The texture maps were calculated by an in-house script written on MATLAB (the Math Works, Inc., Natick, MA, USA) platform. The in-house script was provided in Additional file 1. The key settings of the texture maps calculation were the radius R of a spherical region of interest around each voxel and the maximum distance d for the texture points. In the current study, the R was set as 5 mm, and d was set as 1 mm. The calculation time

of each brain gray matter was 55 s to generate the five texture features maps (Fig. 2).

The positive clusters were saved as masks to extract the texture values, and then were performed correlation analysis with the clinical variables (including VAS score, disease duration, HAMA score, HAMD score, MoCA score).

Statistical analysis

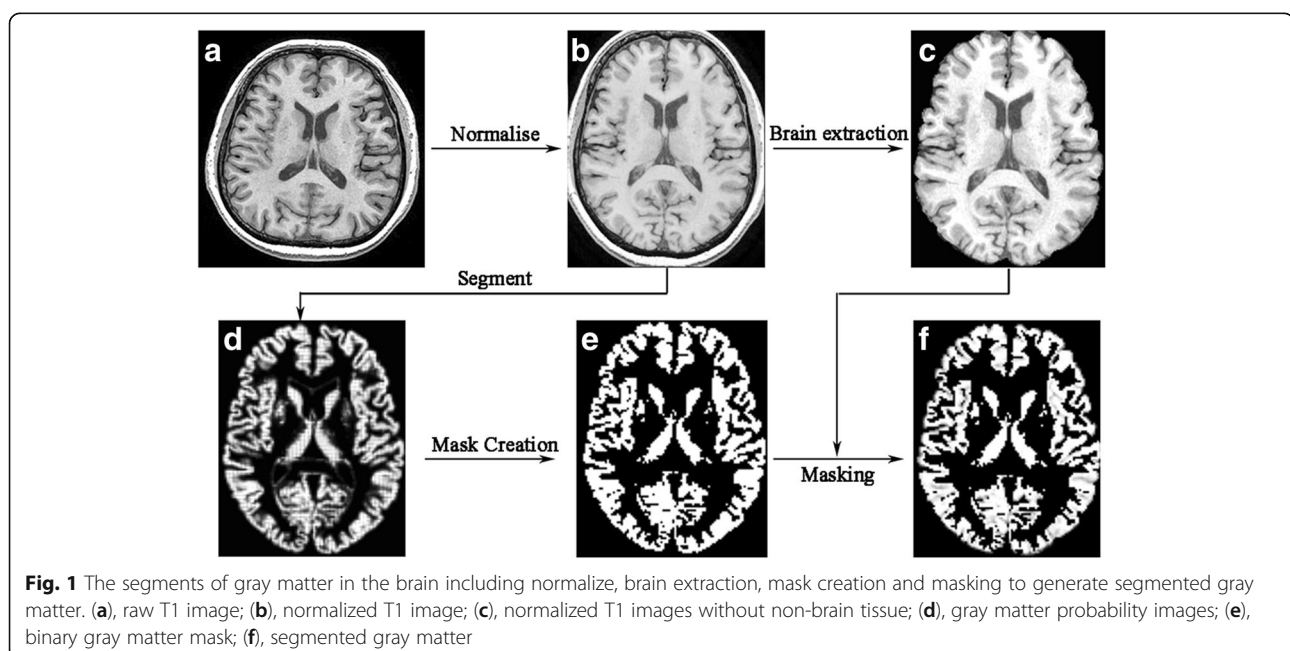
The statistical analysis was performed by using PASW Statistics 18.0. The data with normal distribution was described as mean \pm standard deviation, and performed with independent two-sample t test and Pearson correlation analysis. The data without normal distribution was described as median (P25, P75), and performed with Mann-Whitney U test and Spearman correlation analysis. The qualitative data (such as sex) were performed with Chi-Square test. Significant difference was set at a P value of <0.05 .

Voxel-based texture features analysis over the whole brain was performed between MOH and NC, and two-sample t-test design model was selected to identify the brain regions with significant altered texture features in MOH. Age and gender were considered as covariates, and significance was set at a P value of <0.001 without correction.

Results

Demography and neuropsychological evaluation

Forty-four MOH patients (F/M 36/8) and 32 NC (20/12) were enrolled. Table 1 demonstrated that there was no significant difference for age and sex between MOH and



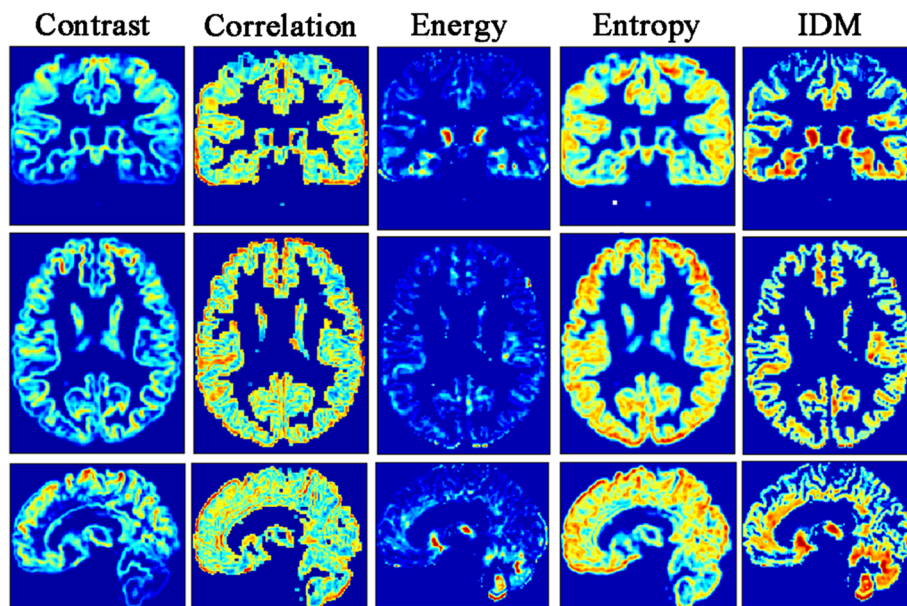


Fig. 2 The texture features maps. 1stcolumn, Contrast map; 2nd column, Correlation map; 3rd, Energy map; 4th, Entropy map; 5th, IDM map

NC. However, significant increased HAMA and HAMD scores and decreased MoCA score were identified in MOH compared with NC ($P < 0.05$).

Voxel-based comparison of contrast map between MOH and NC

Regional increased Contrast located in the right cerebellar Crus and Vermis in MOH compared with NC (Table 2 and Fig. 3). There were no brain regions with decreased Contrast in MOH.

The correlation analysis presented that there was a significant relation with disease duration ($r = 0.31$, P value = 0.04) (Table 3 and Fig. 4). The other texture value of positive clusters showed no significant relation with the clinical variables.

Table 1 The clinical characteristics of MOH patients and normal controls

	MOH	NC	T value	P value
Num(F/M)	44(36/8)	32(20/12)	2.64 ^a	0.10
Age	42.30 ± 9.62	41.34 ± 10.89	0.40	0.69
HAMA	18.25 ± 8.74	10.00(8.25,13.00) ^b	4.24 ^c	0.00
HAMD	19.80 ± 11.85	8.03 ± 4.34	5.34	0.00
MoCA	23.43 ± 3.72	27.16 ± 2.34	5.00	0.00
DD(yrs)	20.00(10.00,20.00) ^b	NA	NA	NA
VAS	8.00(7.25,10.00) ^b	NA	NA	NA

MOH medication-overuse headache, NC normal control, DD disease durationm, VAS Visual Analogue Scale, HAMA Hamilton Anxiety Scale, HAMD Hamilton Depression Scale, MoCA Montreal Cognitive Assessment, NA not available

^aChi-square test

^bMedian (P25, P75)

^cMann-Whitney Z value

Voxel-based comparison of correlation map between MOH and NC

Table 2 demonstrated that the brain regions with increased Correlation located in right parahippocampal gyrus (R-PHG), left middle frontal gyrus (L-MFG) and left dorsolateral periaqueductal gray (L-dlPAG) in MOH patients compared with NC. The decreased Correlation located in right superior parietal lobule (Table 2 and Fig. 5).

Figure 4 presented that there was a negative correlation between the Correlation value of R-PHG and HAMD score ($r = -0.39$, $P = 0.01$). Besides, the Correlation value of R-SPL presented negative relation with disease duration ($r = -0.33$, P value = 0.03), and positive relation with MoCA score ($r = 0.37$, P value = 0.01) (Table 3).

Voxel-based comparison of energy, entropy and IDM map between MOH and NC

The vermis presented decreased Energy and IDM, and increased Entropy in MOH compared with NC (Table 2 and Fig. 6). Left cerebellum exterior also presented decreased Energy in MOH.

The correlation analysis demonstrated there was no any correlation between the texture value of above positive clusters with the clinical variable (Table 3).

Discussion

This is the first study to analyze the brain regions with abnormal texture changes in MOH by using improved voxel-based gray-level co-occurrence matrix (VGLCM) method [20]. Compared with voxel-based morphometry

Table 2 The brain regions with altered texture features over the whole brain between MOH and NC

Texture	BA	Anatomic region	MNI-space			Cluster size	P_{uncorr}	Peak T value
			X	Y	Z			
Contrast								
MOH > NC	NA	Vermis	-3	-47	-18	270	0.000	4.33
	NA	L-cerebellar Crus	-30	-74	-44	158	0.000	3.72
Correlation								
MOH > NC								
	30	R-PHG	18	-30	-14	41	0.000	4.41
	8	L-MFG	-24	17	45	41	0.000	3.74
	NA	L-dIPAG	-2	-30	-9	61	0.000	3.90
MOH < NC								
	7	R-SPL	30	-66	39	51	0.000	3.76
Energy								
MOH < NC								
		Vermis	0	-47	-21	316	0.000	3.87
		L-Cerebellum Exterior	-11	-45	-12	66	0.000	3.64
Entropy								
MOH > NC								
		Vermis	3	-47	-23	438	0.000	4.17
IDM								
MOH < NC								
		Vermis	-2	-47	-20	172	0.000	4.37

L left hemisphere, R right hemisphere, SPL superior parietal lobule, PHG parahippocampal gyrus, MFG middle frontal gyrus, dIPAG dorsolateral periaqueductal gray

to observe the subtle volume changes, this method could detect the fine changes in tissues image intrinsic characteristics with multiple texture parameters mapping and have higher calculation efficacy [20]. Five texture parameters including Contrast, Correlation, Energy (angular second moment, ASM), Entropy and IDM were extracted in this study [15, 18]. Previous studies recognized that Contrast represented the amount of local gray level variation, Correlation represented the linear dependency of grey levels of neighboring pixels, Energy represented image homogeneity, Entropy represented the amount of

information of the image that is needed for the image compression, and IDM represented the local homogeneity [12]. The texture map analyses in the present study revealed altered texture features in cerebellar vermis, left cerebellum, left dorsolateral periaqueductal gray (L-dIPAG), right parahippocampal gyrus (R-PHG), left middle frontal gyrus (L-MFG) and right superior parietal lobule(R-SPL).

The texture parameters of increased Contrast and Entropy, decreased Energy and IDM in cerebellar vermis of MOH patients indicated that the texture feature of

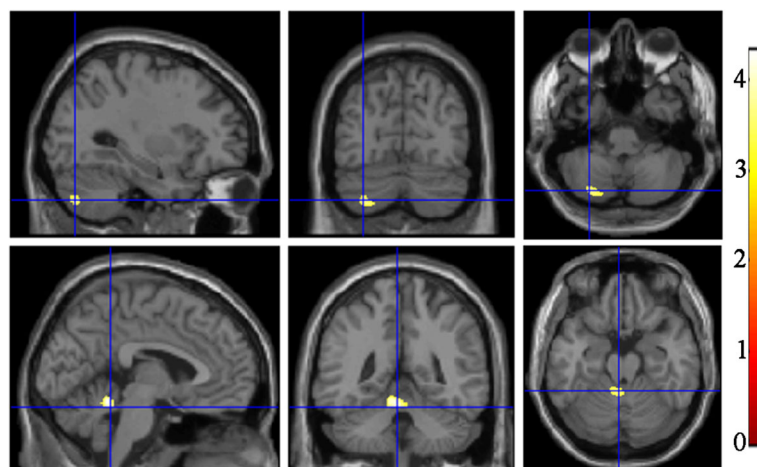


Fig. 3 The brain region with increased Contrast in the left cerebellar Crus and Vermis in MOH compared with NC

Table 3 Correlation analysis between positive clusters' texture value and clinical variables in MOH

Texture	Cluster	Texture value	VAS ^b		DD ^b		HAMA		HAMD		MoCA	
			r value	P value	r value	P value	r value	P value	r value	P value	r value	P value
Contrast												
Increased	L-Cerebellar Crus	1.11(0.69,1.52) ^a	-0.06	0.72	-0.07	0.64	-0.16	0.32	-0.14	0.36	0.27	0.08
	Vermis	1.20 ± 0.46	-0.23	0.14	0.31	0.04	-0.06	0.69	-0.10	0.50	-0.09	0.55
Correlation												
Increased	R-PHG	91.36 ± 23.25	-0.12	0.43	0.05	0.76	-0.23	0.13	-0.39	0.01	0.12	0.43
	L-MFG	77.16(70.31,86.29) ^a	0.22	0.15	0.00	0.98	0.05	0.78	0.15	0.35	0.01	0.96
	L-dIPAG	82.60 ± 7.94	-0.25	0.1	0.19	0.22	-0.11	0.50	-0.13	0.40	-0.01	0.97
Decreased	R-SPL(BA7)	72.58(65.79,78.01) ^a	0.01	0.93	-0.33	0.03	-0.12	0.44	-0.12	0.44	0.37	0.01
Energy												
Decreased	Vermis	36.86 ± 10.03	-0.12	0.43	0.05	0.76	-0.02	0.89	-0.05	0.74	0.03	0.87
	L-Cerebellum Exterior	32.90 ± 10.21	0.22	0.15	0.00	0.98	-0.02	0.88	-0.12	0.44	0.01	0.95
Entropy												
Increased	Vermis	185.71 ± 33.77	-0.07	0.67	0.22	0.16	-0.06	0.69	-0.03	0.87	0.04	0.82
IDM												
Decreased	Vermis	82.32 ± 5.04	0.14	0.37	0.22	0.14	-0.01	0.97	0.02	0.88	0.10	0.54

L left hemisphere, R right hemisphere, SPL superior parietal lobule

^aMedian (P25, P75) with Spearman correlation analysis

^bSpearman correlation analysis

vermis in MOH was more heterogeneous and complicated in MR T1 images. The texture feature of left cerebellum was also more heterogeneous in MOH due to increased Contrast and decreased Energy. The cerebellum has been recently recognized to be associated with cognitive, sensorimotor, pain and affective information processing [24]. In a 18-FDG PET study, cerebellar vermis was hypermetabolic in MOH patients but recovered

to normal 3 weeks after drug withdrawal [25], indicating hypermetabolic status may contribute to increased texture heterogeneity. Patients of familial hemiplegic migraine (FHM) with CACNA1A gene mutation may develop progressive cerebellar signs, and MRI revealed predominant cerebellar vermis atrophy [26] while proton MR spectroscopy (1H-MRS) found reduced NAA, Glu and elevated ml in the superior cerebellar vermis

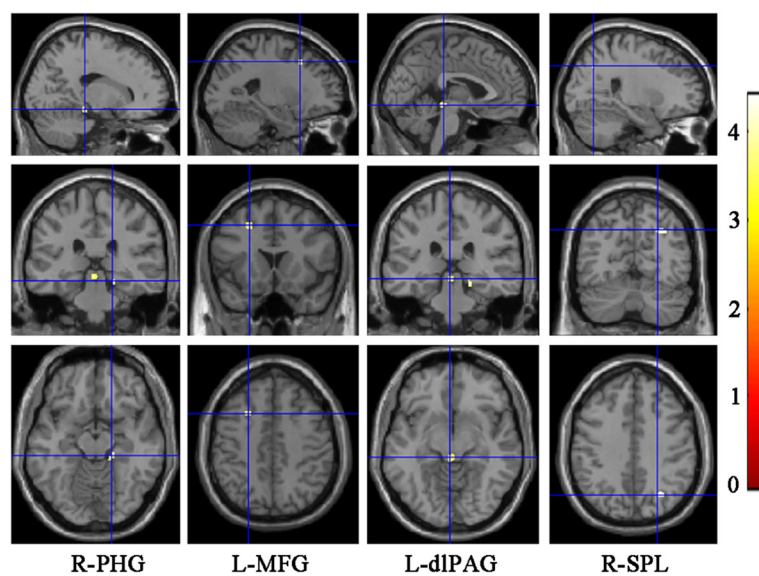
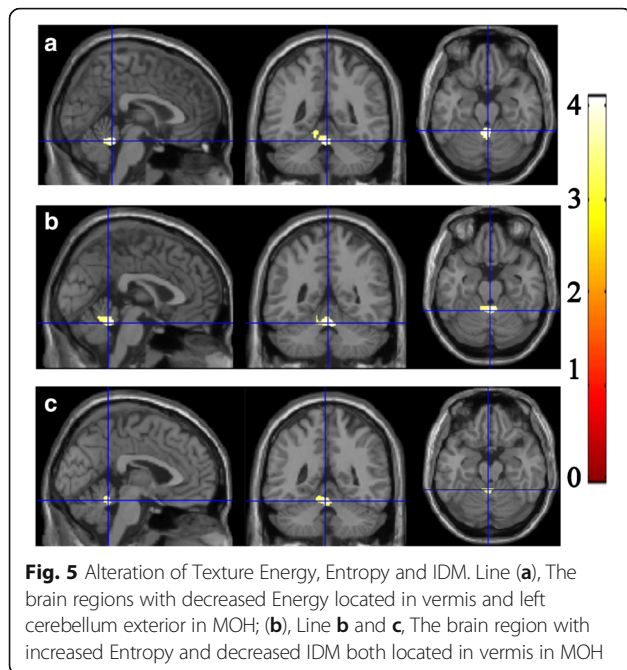


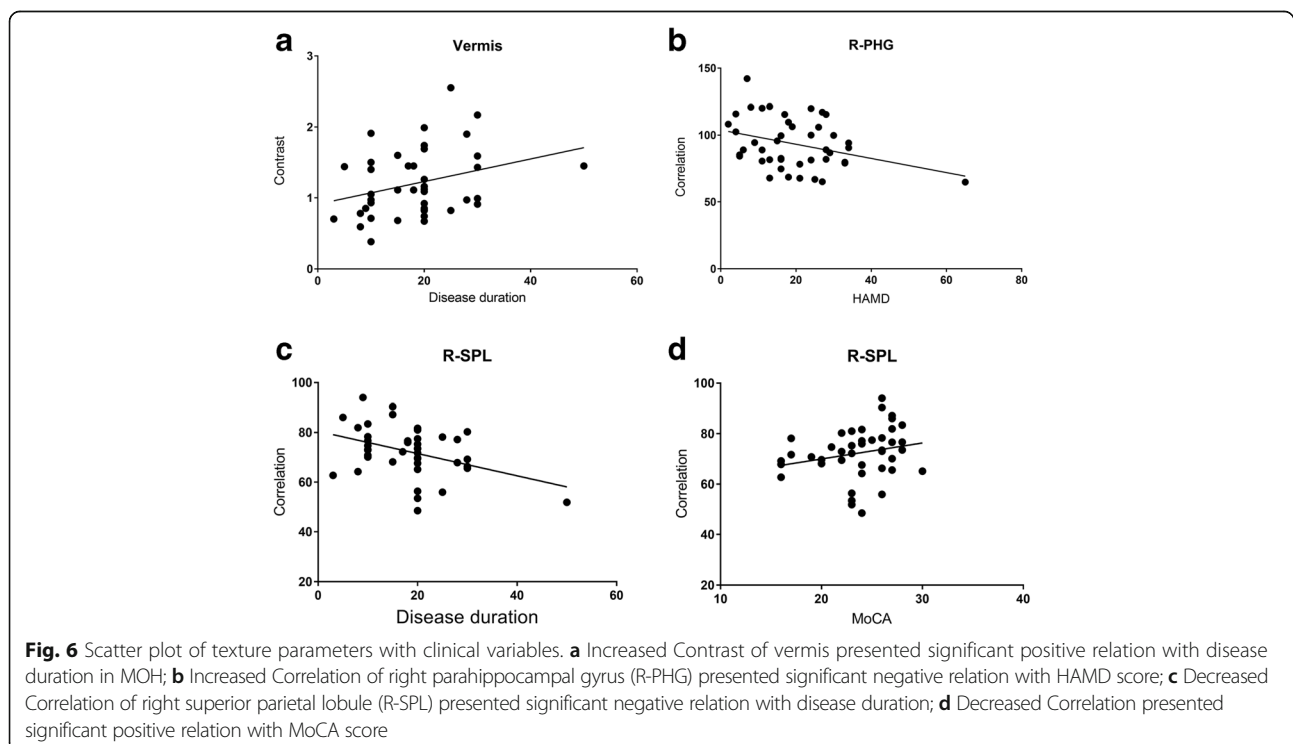
Fig. 4 The increased (1–3 column) and decreased Correlation in MOH compared with normal controls. R, right hemisphere; L, left hemisphere; PHG, parahippocampal gyrus; MFG, middle frontal gyrus; dIPAG, dorsolateral periaqueductal gray; SPL, superior parietal lobule



indicating regionally distinct neuronal impairment [27]. The relationship of FHM and cerebellar vermis atrophy and metabolic abnormality indicated that cerebellar vermis might be genetically vulnerable to injury in migraine patients. Besides, VBM studies found altered grey matter volume of cerebellum and vermis in MOH [28, 29] but not in chronic migraine without medication overuse

[28], supporting that cerebellum was involved in the pathophysiology of MOH. With the evidence of reversible metabolic abnormality of vermis in MOH [25], the change of cerebellar vermis might better be the result of migraine transformation to MOH. The positive correlation of Contrast in vermis with disease duration further suggested the possibility of secondary change of texture feature in genetically vulnerable vermis as a result of migraine chronification with medication overuse. Longitudinal studies would be required to explore this further.

Correlation map in our study demonstrated that increased Correlation located in left dorsolateral periaqueductal gray (L-dIPAG), right parahippocampal gyrus (R-PHG), and left middle frontal gyrus (L-MFG) and decreased Correlation in right superior parietal lobule (R-SPL). A high correlation texture means high predictability of pixel relationships. PAG is considered as a pivotal center in either generation of migraine or in its regulation [30]. Functional and structural MRI studies demonstrated increased iron deposition [31], decreased functional connectivity [9], increased volume [6, 7] and nonspecific hyperintensity lesions [5] of PAG in migraine and MOH patients. Our previous pilot texture analysis using 2D-GLCM found increased contrast in PAG suggesting increased local gray level variation in MR T1 images [7]. The difference of positive texture parameters in PAG may be influenced by the sensitivity of the two different texture analytic methods. However, both texture analyses found changes of texture feature of



PAG and provided evidence of PAG in the pathogenesis of MOH. Like PAG, decreased functional connectivity density of R-PHG was also found in MOH in our previous study [32]. Decreased volume [33] and prolonged T2 relaxation times [34] in R-PHG were identified in smoker and alcohol-use disorders, which suggested R-PHG might participate in the dependence related processing. Gray matter volume reduction of R-PHG was also reported in subthreshold depression [35]. Our study found significantly higher HAMD score in MOH patients and a negative correlation between the Correlation value of R-PHG and HAMD score, which further identified the possible anatomic basis for emotional change and dependence behavior of MOH patients. Altered functional connectivity and grey matter volume of L-MFG [36, 37] and SPL [38, 39] were also found in migraineurs indicating abnormalities in network of pain modulation and discrimination in migraine [39]. A former fMRI study found R-SPL was hypoactive in MOH patients and recovered to almost normal 6 months after drug withdrawal [40], which suggested a modification of the pain network in MOH. In our study, we found that the Correlation value of R-SPL was negatively correlated with disease duration, which further suggested neural plasticity with repetitive pain discrimination in MOH. Furthermore, we found that the Correlation value of R-SPL was positively correlated with MoCA. A recent study using arterial spin-labeled perfusion MRI demonstrated significant positive correlations between cerebral blood flow in SPL and Mini-mental State Examination(MMSE) scores in patients with Alzheimer's disease [41], which suggested a role of SPL in the cognition network.

The current study using an improved VGLCM method can explore whole-brain pathology and brain-behavioral relationships. However, there are several limitations in our study. Firstly, only five texture features were calculated in this study, and more texture features may be considered to screen the significant texture features for MOH patients in the future. Secondly, only 3D high resolution T1-weighted images were used to calculate the texture features, and the other MR images such as T2 weighted image, diffusion weighted image and susceptibility weighted image may also be considered for the texture analysis in the future. Thirdly, dependence behavior was not evaluated in our study and Severity of Dependence Scale (SDS) for MOH patients should be considered for clinical correlation analyses in the future studies. Lastly, longitudinal studies are needed to better identify the dynamic changes of texture feature in MOH.

Conclusions

In conclusion, this study revealed altered texture feature of several brain regions in MOH patients, which may reflect the neural plasticity of pain discrimination and

modulation, affective and cognitive processing in MOH and were helpful in understanding the pathogenesis of MOH. Texture analysis using improved VGLCM method was sensitive and efficient in detecting subtle structural changes over the whole brain in MOH.

Additional file

Additional file 1: The voxel-based gray level co-occurrence matrix (VGLCM) was introduced as follows: Gray level co-occurrence matrix (GLCM) is a well-known statistical texture analysis method in 2D gray level image. It also can be extended to define texture features on 3D gray level image. (DOCX 16 kb)

Abbreviations

dIPAG: Dorsolateral periaqueductal gray; HAMA: Hamilton Anxiety Scale; HAMD: Hamilton Depression Scale; IDM: Inverse difference moment; MFG: Middle frontal gyrus; MoCA: Montreal Cognitive Assessment; MOH: Medication-overuse headache; NC: Normal controls; PHG: Parahippocampal gyrus; SPL: Superior parietal lobule; VAS: Visual analogue scale; VGLCM: Voxel-based gray-level co-occurrence matrix

Acknowledgements

Not applicable

Funding

This work was supported by the Special Financial Grant from the China Postdoctoral Science Foundation (2014 T70960) and the Foundation for Medical and health Sci & Tech innovation Project of Sanya (2016YW37) and National Science Foundation of China (91520202).

Availability of data and materials

All the data supporting our findings is contained within the manuscript.

Authors' contributions

Category 1: (a) Conception and Design: LM; SYY. (b) Acquisition of Data: ZYC; MQL; XYC. (c) Analysis and Interpretation of Data: ZYC, ZQC. Category 2: (a) Drafting the Article: ZYC, XYC. (b) Revising It for Intellectual Content: GHG, LM; SYY. All authors read and approved the final manuscript.

Ethics approval and consent to participate

The Institutional Review Board of the Chinese PLA General Hospital approved the research protocol, and the procedures conformed to the tenets of the Declaration of Helsinki.

Consent for publication

Not applicable

Competing interests

All authors declare that they have no competing interests.

Publisher's Note

Springer Nature remains neutral with regard to jurisdictional claims in published maps and institutional affiliations.

Author details

¹Department of Radiology, Chinese PLA General Hospital, Beijing 100853, China. ²Department of Radiology, Hainan Branch of Chinese PLA General Hospital, Beijing 100853, China. ³Department of Neurology, Chinese PLA General Hospital, Beijing 100853, China. ⁴Research Center for Brain Inspired Intelligence, Institute of Automation, Chinese Academy of Sciences, Beijing 100190, China. ⁵University of Chinese Academy of Sciences, Beijing 100190, China. ⁶Center for Excellence in Brain Science and Intelligence Technology, Beijing 100190, China.

Received: 17 October 2017 Accepted: 13 November 2017

Published online: 28 November 2017

References

- Headache Classification Committee of the International Headache S (2013) The international classification of headache disorders, 3rd edition (beta version). *Cephalalgia* 33:629–808
- Group GBDNDC (2017) Global, regional, and national burden of neurological disorders during 1990–2015: a systematic analysis for the global burden of disease study 2015. *Lancet Neurol*
- Scher AI, Rizzoli PB, Loder EW (2017) Medication overuse headache: an entrenched idea in need of scrutiny. *Neurology* 89:1296–1304
- Diener HC, Holle D, Solbach K, Gaul C (2016) Medication-overuse headache: risk factors, pathophysiology and management. *Nat Rev Neurol* 12:575–583
- Chen Z, Chen X, Liu M, Liu S, Ma L, Yu S (2016) Nonspecific periaqueductal gray lesions on T2WI in episodic migraine. *J Headache Pain*. 17:101
- Chen Z, Chen X, Liu M, Liu S, Ma L, Yu S (2017) Volume gain of periaqueductal gray in medication-overuse headache. *J Headache Pain*. 18:12
- Chen Z, Chen X, Liu M, Liu S, Ma L, Yu S (2017) Volume expansion of periaqueductal gray in episodic migraine: a pilot MRI structural imaging study. *J Headache Pain*. 18:83
- Chen Z, Jia Z, Chen X, Liu M, Liu S, Ma L, Yu S (2017) Volumetric abnormalities of thalamic subnuclei in medication-overuse headache. *J Headache Pain*. 18:82
- Chen Z, Chen X, Liu M, Liu S, Ma L, Yu S (2017) Disrupted functional connectivity of periaqueductal gray subregions in episodic migraine. *J Headache Pain*. 18:36
- Ito K, Kudo M, Sasaki M, Saito A, Yamashita F, Harada T et al (2016) Detection of changes in the periaqueductal gray matter of patients with episodic migraine using quantitative diffusion kurtosis imaging: preliminary findings. *Neuroradiology* 58:115–120
- Zhou SR, Yin JP (2013) LBP texture feature based on Haar characteristics. *Journal of Software* 24:1909–1926
- Mohanaiah P, Sathyanarayana P, Gurukumar L (2014) Image texture feature extraction using GLCM approach. *International Journal of Scientific and Research Publications* 3:1–5
- Gourtsoyianni S, Doumou G, Prezzi D, Taylor B, Stirling JJ, Taylor NJ et al (2017) Primary rectal cancer: repeatability of global and local-regional MR imaging texture features. *Radiology* 284:552–561
- Miles KA, Ganeshan B, Griffiths MR, Young RC, Chatwin CR (2009) Colorectal cancer: texture analysis of portal phase hepatic CT images as a potential marker of survival. *Radiology* 250:444–452
- Wang B, Liu G, Fan W, Zhang X, Lu Y, Chen Z (2017) Value of texture feature analysis in the differential diagnosis of hepatic cyst and Hemangioma in magnetic resonance imaging. *Zhongguo Yi Xue Ke Xue Yuan Xue Bao* 39:169–176
- Sorensen L, Igel C, Pai A, Balas I, Anker C, Lillholm M et al (2017) Differential diagnosis of mild cognitive impairment and Alzheimer's disease using structural MRI cortical thickness, hippocampal shape, hippocampal texture, and volumetry. *Neuroimage Clin* 13:470–482
- Hainc N, Stippich C, Stieltjes B, Leu S, Bink A (2017) Experimental texture analysis in Glioblastoma: a methodological study. *Investig Radiol* 52:367–373
- Chen Z, Chen X, Liu M, Liu S, Ma L, Yu S (2017) Texture features of periaqueductal gray in the patients with medication-overuse headache. *J Headache Pain*. 18:14
- Maani R, Yang YH, Kalra S (2015) Voxel-based texture analysis of the brain. *PLoS One* 10:e0117759
- Maani R, Yang YH, Emery D, Kalra S (2016) Cerebral degeneration in amyotrophic lateral sclerosis revealed by 3-dimensional texture analysis. *Front Neurosci* 10:120
- Maier W, Buller R, Philipp M, Heuser I (1988) The Hamilton anxiety scale: reliability, validity and sensitivity to change in anxiety and depressive disorders. *J Affect Disord* 14:61–68
- Hamilton M (1967) Development of a rating scale for primary depressive illness. *Br J Soc Clin Psychol* 6:278–296
- Chen Z, Li L, Sun J, Ma L (2012) Mapping the brain in type II diabetes: voxel-based morphometry using DARTEL. *Eur J Radiol* 81:1870–1876
- Timmann D, Drepper J, Frings M, Maschke M, Richter S, Gerwig M, Kolb FP (2010) The human cerebellum contributes to motor, emotional and cognitive associative learning. A review *Cortex* 46:845–857
- Fumal A, Laureys S, Di Clemente L, Boly M, Bohotin V, Vandenheede M et al (2006) Orbitofrontal cortex involvement in chronic analgesic-overuse headache evolving from episodic migraine. *Brain* 129:543–550
- Wada T, Kobayashi N, Takahashi Y, Aoki T, Watanabe T, Saitoh S (2002) Wide clinical variability in a family with a CACNA1A T666m mutation: hemiplegic migraine, coma, and progressive ataxia. *Pediatr Neurol* 26:47–50
- Dichgans M, Herzog J, Freilinger T, Wilke M, Auer DP (2005) 1H-MRS alterations in the cerebellum of patients with familial hemiplegic migraine type 1. *Neurology* 64:608–613
- Lai TH, Chou KH, Fuh JL, Lee PL, Kung YC, Lin CP, Wang SJ (2016) Gray matter changes related to medication overuse in patients with chronic migraine. *Cephalalgia* 36:1324–1333
- Riederer F, Marti M, Luechinger R, Lanzenberger R, von Meyenburg J, Gantenbein AR et al (2012) Grey matter changes associated with medication-overuse headache: correlations with disease related disability and anxiety. *World J Biol Psychiatry* 13:517–525
- Knight YE, Goadsby PJ (2001) The periaqueductal grey matter modulates trigeminovascular input: a role in migraine? *Neuroscience* 106:793–800
- Welch KM, Nagesh V, Aurora SK, Gelman N (2001) Periaqueductal gray matter dysfunction in migraine: cause or the burden of illness? *Headache* 41:629–637
- Chen Z, Chen X, Liu M, Dong Z, Ma L, Yu S (2017) Altered functional connectivity architecture of the brain in medication overuse headache using resting state fMRI. *J Headache Pain*. 18:25
- Ding X, Yang Y, Stein EA, Ross TJ (2015) Multivariate classification of smokers and nonsmokers using SVM-RFE on structural MRI images. *Hum Brain Mapp* 36:4869–4879
- Bagga D, Modi S, Poonia M, Kaur P, Bhattacharya D, Garg ML et al (2015) T2 relaxation time alterations underlying neurocognitive deficits in alcohol-use disorders (AUD) in an Indian population: a combined conventional ROI and voxel-based relaxometry analysis. *Alcohol* 49:639–646
- Zhou H, Li R, Ma Z, Rossi S, Zhu X, Li J (2016) Smaller gray matter volume of hippocampus/parahippocampus in elderly people with subthreshold depression: a cross-sectional study. *BMC Psychiatry* 16:219
- Hougaard A, Amin FM, Larsson HB, Rostrup E, Ashina M (2017) Increased intrinsic brain connectivity between pons and somatosensory cortex during attacks of migraine with aura. *Hum Brain Mapp* 38:2635–2642
- Jia Z, Yu S (2017) Grey matter alterations in migraine: a systematic review and meta-analysis. *Neuroimage Clin*. 14:130–140
- Amin FM, Hougaard A, Magon S, Sprenger T, Wolfram F, Rostrup E, Ashina M. (2017) Altered thalamic connectivity during spontaneous attacks of migraine without aura: a resting-state fMRI study. *Cephalalgia*.333102417729113
- Zhang J, YL W, Su J, Yao Q, Wang M, Li GF et al (2017) Assessment of gray and white matter structural alterations in migraineurs without aura. *J Headache Pain* 18:74
- Grazzi L, Chiapparini L, Ferraro S, Usai S, Andrasik F, Mandelli ML et al (2010) Chronic migraine with medication overuse pre-post withdrawal of symptomatic medication: clinical results and fMRI correlations. *Headache* 50:998–1004
- Kaneta T, Katsuse O, Hirano T, Ogawa M, Shihikura-Hino A, Yoshida K et al (2017) Voxel-wise correlations between cognition and cerebral blood flow using arterial spin-labeled perfusion MRI in patients with Alzheimer's disease: a cross-sectional study. *BMC Neurol* 17:91

Submit your manuscript to a SpringerOpen® journal and benefit from:

- Convenient online submission
- Rigorous peer review
- Open access: articles freely available online
- High visibility within the field
- Retaining the copyright to your article

Submit your next manuscript at ► springeropen.com